frontiers | Frontiers in Marine Science

TYPE Original Research
PUBLISHED 03 November 2022
DOI 10.3389/fmars.2022.1027561

Check for updates

OPEN ACCESS

EDITED BY
Zhaohui Zhang,
Zhejiang University, China

REVIEWED BY
Zeynep Erdem,
Royal Netherlands Institute for Sea Research (NIOZ), Netherlands
Ding He,
Hong Kong University of Science and Technology, Hong Kong SAR, China

*CORRESPONDENCE
Lei Xing
xinglei@ouc.edu.cn
Rui Bao
baorui@ouc.edu.cn

SPECIALTY SECTION
This article was submitted to Marine Biogeochemistry, a section of the journal Frontiers in Marine Science

RECEIVED 25 August 2022
ACCEPTED 17 October 2022
PUBLISHED 03 November 2022

CITATION
Song C, Dang T, Zhang T, Ge T, Xiang R, Xing L, Bao R, Zhou Y, Xiao R and Wu B (2022) Evolutions of upwelling and terrestrial organic matter input in the inner shelf of the East China Sea in the last millennium revealed by long-chain alkyl diols proxies.
Front. Mar. Sci. 9:1027561.
doi: 10.3389/fmars.2022.1027561

Evolutions of upwelling and terrestrial organic matter input in the inner shelf of the East China Sea in the last millennium revealed by long-chain alkyl diols proxies

Chuanhui Song[1,2], Tianxiang Dang[1,2], Ting Zhang[1], Tiantian Ge[1], Rong Xiang[3], Lei Xing[1,2]*, Rui Bao[1,2]*, Yang Zhou[1,2], Rui Xiao[1,2] and Baojin Wu[1,2]

[1]Key Laboratory of Marine Chemistry Theory and Technology, Ministry of Education, Ocean University of China, Qingdao, China, [2]Laboratory for Marine Ecology and Environmental Science, Qingdao National Laboratory for Marine Science and Technology, Qingdao, China, [3]Key Laboratory of Ocean and Marginal Sea Geology, South China Sea Institute of Oceanology, Chinese Academy of Sciences, Guangzhou, China

Long-chain alkyl diols (LCDs) can be used as organic geochemical proxies for paleoceanographic change, especially in marginal sea areas where large volumes of sediments are deposited rapidly and continuously. However, little is known about the applicability and response on a millennium scale in relation with existing records in those sediments. We reconstruct changes in upwelling and terrestrial organic matter (OM) input in core sediments from the Zhejiang Fujian coastal station (T08) and Yangtze River Estuary station (T06) in the inner shelf of the East China Sea (ECS) over the last millennium, using the LCD based proxies: diol index 2 (DI-2), and FC_{32}1,15-diol. Our results show that DI-2 values ([(C_{28}+C_{30})1,14-diols]/([(C_{28}+C_{30})1,13-diols]+[(C_{28}+C_{30})1,14-diols])) at T08 decrease significantly during 600−400 yr BP but increase gradually after 400 yr BP. The FC_{32}1,15-diol proxy ([C_{32}1,15-diol]×100/([(C_{28}+C_{30})1,13-diols]+[(C_{30}+C_{32})1,15-diols])) at T06 shows marked fluctuations during 1000−800 yr BP, followed by a significant decline during 800−500 yr BP but a subsequent increase from 500 to 300 yr BP. We find that variations in DI-2 values are broadly consistent with changes in the strength of the East Asian Summer Monsoon (EASM) and the Kuroshio Current and are likely linked to changes in the frequency and intensity of the El Niño-Southern Oscillation (ENSO). The increased strength of the EASM causes greater offshore movement of the upper layer of seawater, which in turn triggers upwelling of bottom waters formed by Kuroshio subsurface waters. We find that variations in FC_{32}1,15-diol proxy are controlled mainly by the East Asian Winter Monsoon (EAWM) and the Yangtze River discharge. By increasing the strength of the EAWM, southward transportation of material deposited in the estuary of the Yangtze River by the ECS coastal currents is promoted. In addition, we synthesize records of other organic geochemical indicators nearby core sediments in the ECS; these records emphasize the importance of reconstructing the evolutionary history of upwelling and subdividing the relative inputs of terrestrial OM. Our study provides a new means for reconstructing the evolution of upwelling and terrestrial OM input in the inner shelf of the ECS over the last millennium.

KEYWORDS

long-chain alkyl diols, upwelling intensity, terrestrial organic matter input, inner shelf of the East China Sea, Late Holocene

1 Introduction

Long chain alkyl diols (LCDs), which are composed of a long alkyl chain containing groups at C_1 and a mid-chain position (Versteegh et al., 1997), are biomarkers that have been used as palaeoenvironmental proxies (e.g., Lattaud et al., 2017a; Zhu et al., 2018). The 1,13- and 1,15-diols are produced by eustigmatophyte algaes, which are mainly freshwater species (Rampen et al., 2014a), and only a few exist in the marine environment (Balzano et al., 2018; Rampen et al., 2022). It has been found that C_{32}1,15-diol content is higher in areas strongly influenced by river runoff and lower in relatively open marine environments (Versteegh et al., 1997; Rampen et al., 2014a), leading to the suggestion that this diol is produced *in situ* in rivers (de Bar et al., 2016). As a result, the riverine organic matter (OM) input index FC_{32}1,15-diol, which is based on relative C_{32}1,15-diol content, is proposed and successfully applied to reconstruct the evolutionary history of riverine OM input over the Quaternary (Lattaud et al., 2017a; Lattaud et al., 2017b). The calculation is based on the following equation:

$$FC_{32}1,15-diol = [C_{32}1,15-diol] \times 100/([(C_{28}+C_{30})1,13-diols]+[(C_{30}+C_{32})1,15-diols]) \quad (1)$$

1,14-diols are commonly found in marine sediments. The biological sources of 1,14-diols are *Proboscia* diatoms, which are often abundant in upwelling regions (Sinninghe Damsté et al., 2003; Rampen et al., 2007; Rampen et al., 2008). Two diol proxies (DI) based on the relative ratios of 1,14-diols to non-upwelling diols, DI-1 and DI-2, were proposed to quantify upwelling intensities in the Arabian Sea (Rampen et al., 2008) and the Antarctic (Willmott et al., 2010), respectively. The DI-1 and DI-2 are calculated as follows:

$$Diol\ \ indx\ \ 1 = [(C_{28}+C_{30})1,14-diols]/([(C_{28}+C_{30})1,14-diols]+[C_{30}1,15-diol]) \quad (2)$$

$$Diol\ \ indx\ \ 2 = [(C_{28}+C_{30})1,14-diols]/([(C_{28}+C_{30})1,13-diols]+[(C_{28}+C_{30})1,14-diols]) \quad (3)$$

Later studies revealed that abundances of C_{30}1,15-diol in DI-1 index were more sensitive to changes in annual mean sea surface temperature than those of 1,13-diols in DI-2 index (Rampen et al., 2012). DI-1 values were also shown significantly correlated with nutrient (N, P and Si) concentrations (Rampen et al., 2012). As result, DI-2 index are less subjected to the influence from environmental factors, and can be applied in reconstructing coastal upwelling intensities.

The East China Sea (ECS) is an important marginal sea influenced by the Yangtze River discharge, which inputs 2–5 Mt/yr of particulate organic carbon (POC) and 0.9 Mt/yr of dissolved organic carbon (DOC) to the ECS every year (Wu et al., 2007). The high concentrations of POC are possibly related to particulate OM input from local vegetation sources and OM produced *in situ* in the river (Wu et al., 2007). The OM, which is delivered by the Changjiang Diluted Water (CDW), enters the shallow sea and is transported southward along the Zhejiang Fujian Coastal Current (ZFCC) in winter (Beardsley et al., 1985; Hu, 1994; Wang, 1998; Wang et al., 2008). Its passage is then blocked by the Taiwan Warm Current (TWC), causing deposition in the coastal zone and forming the depocenter in the inner shelf of the ECS (Guo et al., 2003; Liu et al., 2007). Under the influence of the CDW, the ECS near the Yangtze River Estuary (YRE) is significantly influenced by river input (Liu et al., 2007), which makes it an excellent location for the application of proxy for riverine OM input.

Furthermore, due to the shoreward invasion of Kuroshio subsurface water (KSSW), there is all-year-round coastal upwelling in the ECS (Mao et al., 1964; Hu et al., 1980; Ding, 1983; Xu, 1986; Luo and Yu, 1998; Jing et al., 2007), making it a suitable location for investigating past changes in coastal upwelling. In summer, southerly winds prevail along the Zhejiang and Fujian coasts, causing an increase in upwelling intensity (Jing et al., 2007). Moreover, during El Niño-like states, enhanced local wind stress leads to intensified upwelling and high nutrient content in surface waters (Zhu et al., 2018). However, due to the lack of proxy

10.3389/fmars.2022.1027561

indicating the past changes in upwelling intensity, the evolutionary history of the coastal upwelling system in the ECS since the Late Holocene still remains unclear.

In this study, we analyze the compositional changes of LCDs in sediments from two cores (Figure 1) spanning the past 1000 years from the depocenter in the inner shelf of the ECS. Diol proxies are used to reconstruct upwelling intensity in the coastal upwelling areas of Zhejiang and Fujian and riverine OM input in the YRE. Combined with other palaeoenvironmental records, we conduct a preliminary investigation into the mechanisms behind environmental changes in the upwelling area along the Zhejiang and Fujian coast and the area closer to the YRE.

2 Samples and methods

2.1 Regional environment and sampling

The ZFCC, the TWC, the KSSW, and the CDW make up the circulation system of the ECS (Lee and Chao, 2003; Wu et al., 2018; Figure 1). The coastal areas of Zhejiang and Fujian in the ECS are mainly influenced by upwelling, which is caused by the combined effects of the southeasterly monsoon and the KSSW (Lie et al., 2003; Yang et al., 2011). Numerical model has shown that phosphorus-rich deep water is transported to the coastal areas of Zhejiang and Fujian by the KSSW before being upwelled to the surface water off the coast of Zhejiang (Yang et al., 2013), enhancing the primary production in the region. The process is enhanced by a strong southeasterly monsoon (Lie et al., 2003). The nearby YRE areas of the ECS are mainly influenced by the CDW. In summer, the CDW expands mainly to the northeast of the ECS, while CDW moves mostly southward along the shore in winter (Wang, 1998).

Cores T06 (122.671°E, 29.499°N, water depth 49 m) and T08 (122.472°E, 28.504°N, water depth 65 m) were recovered from the northern part of the depocenter of the ECS inner shelf (Figure 1). The cores were collected using gravity corers on the *R/V Dong Fang Hong 2* in 2011 during the Project 973 Cruise. All samples were stored at −20°C before analysis.

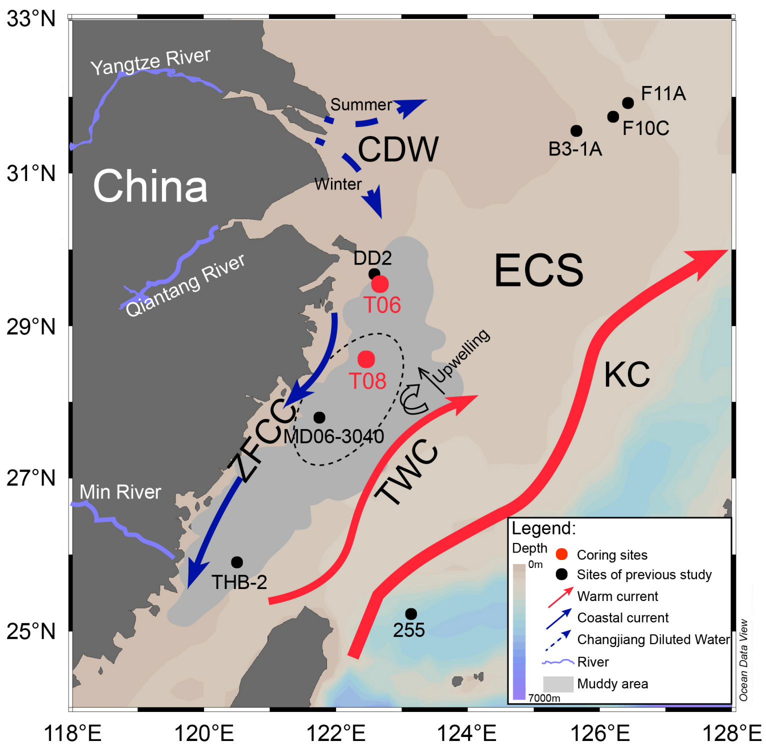

FIGURE 1
A map showing the locations of cores T06 and T08 and the circulation system in the ECS. The area marked by the gray shadow represents the depocenter of the ECS inner shelf and we use the following abbreviations: Kuroshio Current—KC; Taiwan Warm Current—TWC; Zhejiang Fujian Coastal Current—ZFCC; Changjiang Diluted Water—CDW. 255, THB-2, MD06-3040, DD2, B3-1A, F10C, and F11A denote the cores from which we compile data for comparison with our records. The black dashed circle represents main upwelling cell (Liu et al., 2007). (A detailed list of abbreviations and references to previous studies can be found in Supplementary Materials).

2.2 Sample analyses

2.2.1 Radiocarbon dating and age model reconstruction

About 15–20 mg mixed benthic foraminifera (mainly are *Ammonia Compressiuscula* and *Ammonia ketienziensis*) were picked out from six horizons in cores T06 and T08 for AMS (accelerator mass spectrometry) ^{14}C dating at Beijing University. The radiocarbon dates were converted to calendar ages using the Calib6.1.1 program (Stuiver and Reimer, 2016), with the local marine reservoir correction (ΔR) set to −128 ± 35 year (Kong and Lee, 2005). The age model was established by linear interpolation between calibrated ages. The base of the 247-cm-long T08 core was dated to 3589 yr BP, and the base of the 270-cm-long T06 core was dated to 9036 yr BP. Dating data of two cores are shown in Supplementary Materials (S1). Since LCDs measurement required a large number of samples and the study mainly focused on the changes in the late Holocene, the T08 core was sampled at 5 cm and the front section of the core samples (120 cm) was analyzed (about the past 1010 yr BP); the T06 core was sampled at 2 cm, and the front section of core samples (40 cm) was analyzed (about the past 1050 yr BP). The ^{14}C age mode of core T08 has been reported by Wu et al. (2018). The ^{14}C data of core T06 indicate that the sedimentary rate of the front section (40 cm) is about 0.049 cm/yr over the last 1000 years, closed to that of the adjacent core PC-6 (122.567°E, 28.968°N; about 0.054 cm/yr; Xiao et al., 2005).

2.2.2 Biomarker analysis

About 10 g freeze dried samples were grounded, and the internal standards (n-$C_{24}D_{50}$ and n-$C_{19}H_{39}OH$) were added. They were extracted ultrasonically 8 times with dichloromethane (DCM): methanol (MeOH; 3:1, v:v), followed by centrifuging. After that, all extracts were combined, dried under an N_2 stream, hydrolyzed with 6% KOH–MeOH solution and extracted into n-hexane. The neutral lipids were purified using silica gel chromatography by elution with DCM : MeOH (95:5, v:v). The fraction containing alcohols was converted to derivative with N,O-bis(trimethylsilyl)-trifluoroacetamide (BSTFA) at 70 ° C for 1 h prior to analyzing.

Qualitative analysis of the biomarkers was performed using gas chromatography–mass spectrometry tandem instrument (GC–MS–MS, Agilent 7890A-G70001B). Separation was achieved with a 30 m × 0.25 mm capillary column (HP-5MS) coated with 0.32 µm film thickness and He as the carrier gas at 2 mL/min. Oven temperature programming was 70–130 °C at 20 °C/min, 130–310 °C at 4 °C/min, and holding at 310 °C for 15 min. The ion source was operated in the electron ionization (EI) mode at 70 EV, and the full scan mode was analyzed in the m/z range of 50–600 amu. Single ion monitoring (SIM) method was carried out according to the characteristic ion mass charge ratio of different diols (de Bar et al., 2017).

3 Results

Four LCDs were detected in the sediment samples from core T06 (Figure 2A). C_{30}1,15-diol was present in the highest concentrations (accounting for 57%–74% of total diols, average = 64%, n = 21) followed by C_{28}1,14-diol (9%–30%, average = 19%, n = 21), C_{32}1,15-diol (8.8%–20%, average = 14%, n = 21), and finally C_{28}1,13-diol (0%–8.8%, average = 3.9%, n = 21). Six LCDs were detected in sediment samples from core T08 (Figure 2B). Again, C_{30}1,15-diol was the major diol in this core (accounting for 65%–79% of total diols, average = 72%, n = 22) followed by C_{32}1,15-diol (7%–12%, average = 9.4%, n = 22), C_{28}1,14-diol (3.9%–15%, average = 8.9%, n = 22), C_{30}1,14-diol (3.4%–7.1%, average = 5.2%, n = 22), and finally the 1,13-diols (1.4%–4.0%, average = 2.3% for C_{30}1,13-diol; 0.4%–3.2%, average = 2.0% for C_{28}1,13-diol, n = 22). Overall, the distribution of LCDs in the sediments from cores T06 and T08 shows that C_{30}1,15-diol is the dominant component, 1,14-diols are the second most abundant, and 1,13-diols are present in the lowest proportions, which is consistent with what is known about the surface sediments of the ECS (He et al., 2020).

It is noteworthy that mono-unsaturated 1,14-diols are not detected in sediment samples from cores T06 or T08. The reason may be that the degradation of mono-unsaturated 1,14-diols is preference to saturated 1,14-diols (Rampen et al., 2014b). Moreover, previous study in the surface sediments of the ECS showed that nutrient diol index (NDI) based on 1,14-diols did not correlate well with nutrient concentrations, which may be related to the increase in silicate content due to nutrient input from freshwater such as the Yangtze River (He et al., 2020). This nutrient structure would hinder the growth of *Proboscia* diatoms which biosynthesize the 1,14-diols (Sinninghe Damsté et al., 2003).

4 Discussion

4.1 Evolution of upwelling intensity based on DI-2 proxy

The $\delta^{13}C$ of total organic carbon ($\delta^{13}C_{TOC}$) is readily influenced by sources (Hedges et al., 1997), plant type (Goñi et al., 1998) and microbial OM contribution (O'Leary, 1988). The $\delta^{13}C$ values in aquatic algae are around -20‰, while the average $\delta^{13}C$ values is -27‰ in terrestrial C_3 plants and -14‰ in terrestrial C_4 plants (Meyers, 1997). Previous studies have demonstrated that Yangtze River is the main source of terrestrial input along the Zhejiang coast, and the C_3 plants dominates throughout the entire basin (Wu et al., 2007). Therefore, the variations in $\delta^{13}C_{TOC}$ values reflect the relative contribution of marine OM to C_3 plants in the study area. More positive $\delta^{13}C_{TOC}$ values indicate higher marine OM contribution

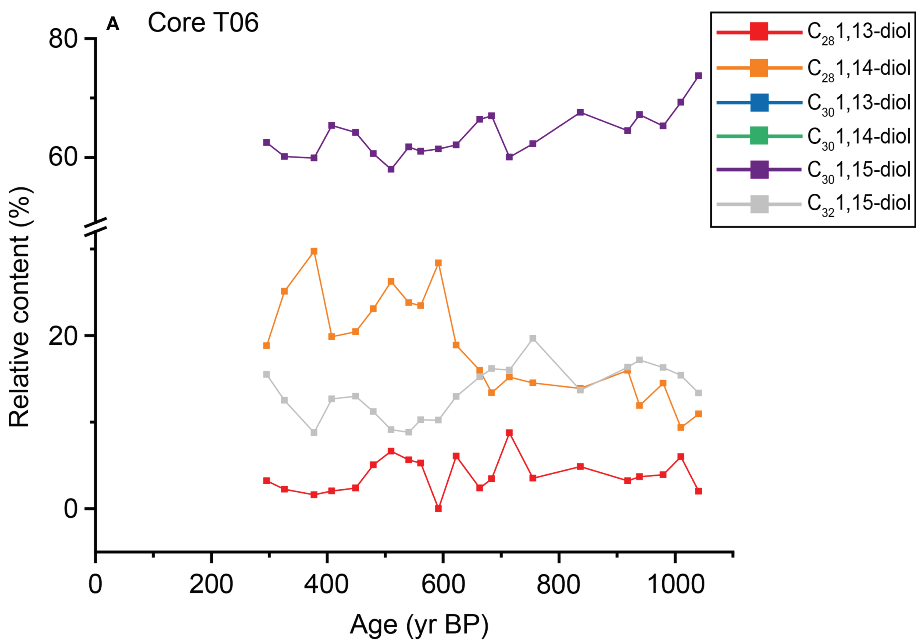

FIGURE 2
Downcore variations in the relative contents of various diols species in sediment samples from **(A)** core T06 and **(B)** core T08. The contents of C_{30}1,13-diol and C_{30}1,14-diol are below the detection limit in core T06.

or marine productivity. In core T08, during the 1000–600 yr BP, the DI-2 values slightly decline within the range from 0.74 to 0.71, which we interpret as a relatively decreased marine productivity, as the $\delta^{13}C_{TOC}$ values vary from −21.9‰ to −22.1‰ (Wu et al., 2018; Figures 3B, C). The lowest DI-2 values and the most negative $\delta^{13}C_{TOC}$ values indicate low contribution of marine OM over the period of 600–400 yr BP, and the positive trend in DI-2 values and $\delta^{13}C_{TOC}$ values indicate enhanced marine OM contribution during the 400–100 yr BP (Wu et al., 2018; Figures 3B, C). We consider that the DI-2 proxy in core T08 reflects productivity changes and, therefore, upwelling intensity.

Based on the variations in DI-2 values in core T08, we divide the time series into three periods: Period I (1000–600 yr BP),

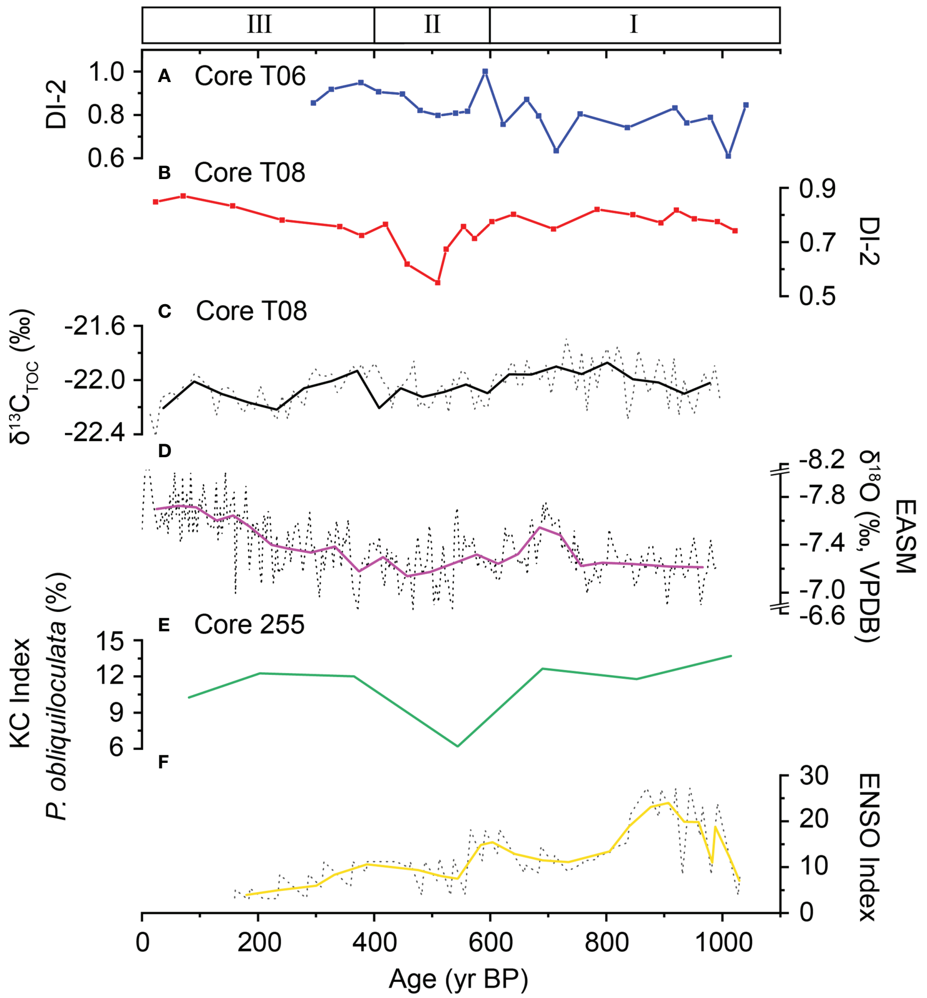

FIGURE 3
Records of DI-2 values in cores T06 and T08 and other environmental indicators over the past 1000 years: **(A)** DI-2 proxy record from core T06; **(B)** DI-2 proxy record from core T08; **(C)** $\delta^{13}C_{TOC}$ record from core T08, the solid line indicates a 5-point average (Wu et al., 2018); **(D)** EASM record reconstructed from oxygen isotope ratios ($\delta^{18}O$) of stalagmites in Dongge Cave, the solid line indicates a 10-point average (Wang et al., 2005); **(E)** Holocene KC index from the Northwest Pacific reconstructed from the abundance of the KC indicator *Pulleniatina obliquiloculata* in core 255 (Jian et al., 2000); and **(F)** ENSO index over the last millennium based on the event model, the solid line indicates a 5-point average (Moy et al., 2002).

Period II (600–400 yr BP), and Period III (400 yr BP to the present). During Period I, the DI-2 values change slightly, fluctuating within the range of 0.74–0.82 with an average value of 0.78 (n = 10; Figure 3B). Analysis of the oxygen isotope ratios ($\delta^{18}O$) of stalagmites in Dongge Cave, indicates the relatively steady intensity of East Asian Summer Monsoon (EASM) in the period I (Wang et al., 2005; Figure 3D). The relatively constant values in the abundance of planktonic foraminifer *Pulleniatina obliquiloculata* during the period I, suggest a steady Kuroshio Current (KC) intensity at that time (Jian et al., 2000; Figure 3E). During period II, the DI-2 values decrease significantly, reaching the lowest value (0.55) at 500 yr BP, when the EASM and KC also weaken (Jian et al., 2000; Wang et al., 2005; Figures 3B, D, E). During Period III, the strength of the EASM gradually increases but the KC intensity is relatively steady, and the DI-2 values show an increasing trend (Jian et al., 2000; Wang et al., 2005; Figures 3B, D, E). In summary, these records indicate that the variations in EASM and the KC control the intensity of coastal upwelling in the ECS since the last 1000 years. This is consistent with modern investigation on coastal upwelling of the ECS (Jing et al., 2007; Yang et al., 2011; Yang et al., 2013). In addition, global climate fluctuations can affect regional variations in upwelling intensity. Downcore fluctuations in DI-2 values from core T08 show similar characteristics to records of El Niño-Southern Oscillation (ENSO) over the last millennium (Moy et al., 2002; Figures 3B, F), suggesting that an increase in the frequency and intensity of ENSO events may result in an increase in upwelling intensity along the Zhejiang and Fujian coasts in the ECS. Previous investigations have shown that ENSO is responsible for variations in local wind stress and thus upwelling intensity, and that strong upwelling events occur after strong El Niño warm events (Kuo et al., 2004; Hong et al., 2009; Zhu et al., 2018). This suggests that the influence of ENSO events on the DI-2 proxy in this area of the ECS cannot be excluded.

It is noteworthy that the DI-2 values in core T06 are not consistent with the trends seen in records of the EASM strength and the KC intensity. For example, during Period II, both the strength of the EASM and the KC decrease significantly (Jian et al., 2000; Wang et al., 2005), while the DI-2 values in core T06 show a slight increase (Figures 3A, D, E). This is likely that at T06, the contents of C_{30}1,13-diol and C_{30}1,14-diol are below the detection limit, and the low C_{28}1,13-diol content may have led to large deviations in the calculated DI-2 values. Hence, the DI-2 index is not applicable at T06 station.

4.2 Reconstructing the history of terrestrial OM input using the FC_{32}1,15-diol proxy

Based on variations in FC_{32}1,15-diol proxy in core T06, we identify three periods: Period I (1000–800 yr BP), Period II (800–500 yr BP), and Period III (500–300 yr BP). During Period I, FC_{32}1,15-diol values increase and then decrease, fluctuating within the range of 14.98–19.52, with an average value of 17.65 (n = 6; Figure 4A). East Asian Winter Monsoon (EAWM) records reconstructed with average particle size in the<45 μm size fraction in core DD2 indicate a relatively strong and then weakened EAWM during Period I (Xiao et al., 2004; Figures 1, 4C). During Period II, the FC_{32}1,15-diol values decline significantly, and the minimum value (11.56) occurs at about 540 yr BP, when the strength of the EAWM also decreases (Xiao et al., 2004; Figures 4A, C). During Period III, the FC_{32}1,15-diol values increase, consistent with the strengthening variations in Yangtze River discharge and the EAWM (Xiao et al., 2004; Wang et al., 2014; Figures 4A, C, D). The enhanced runoff from the

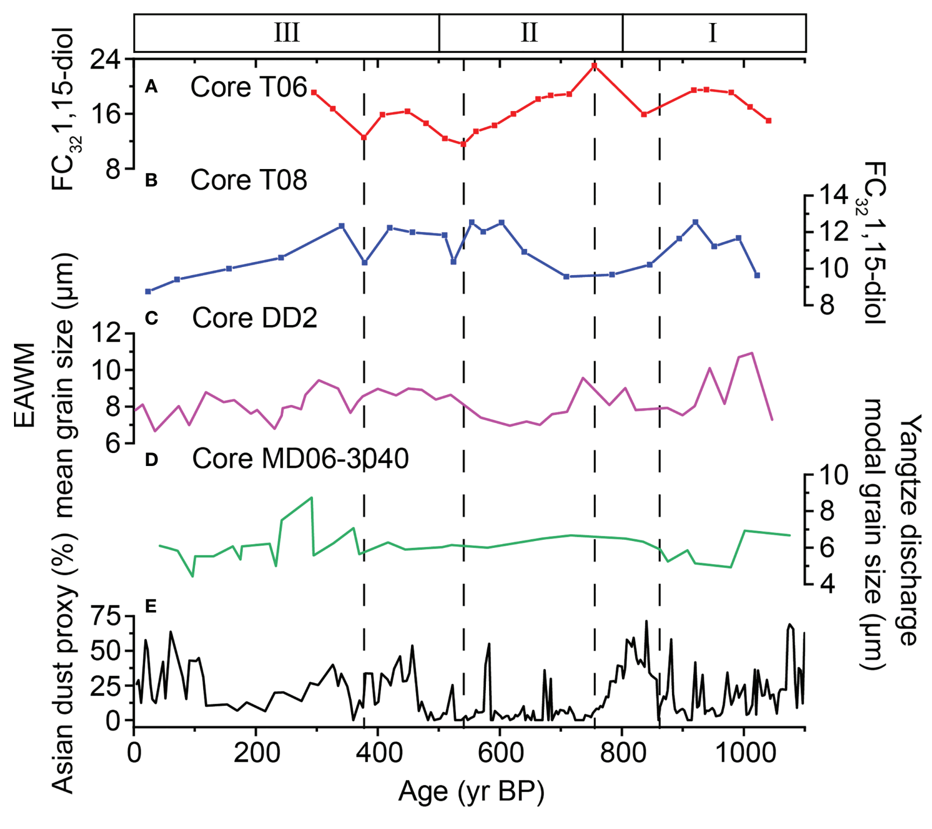

FIGURE 4
Records of FC_{32}1,15-diol proxy in cores T06 and T08 and other environmental parameters over the past 1000 years: **(A)** FC_{32}1,15-diol proxy in core T06; **(B)** FC_{32}1,15-diol proxy in core T08; **(C)** EAWM strength, as reconstructed from average particle size in the<45 μm size fraction in core DD2 (Xiao et al., 2004); **(D)** Yangtze River discharge, as inferred from the modal grain size of the fine silt fraction from core MD06-3040 (Wang et al., 2014); and **(E)** changes in Asian dust activity, as inferred from Lake Gonghai, northern China (Chen et al., 2020). The black dashed line indicates that the main phases of increased FC_{32}1,15-diol values at T06 correspond well to increases in Asian dust emissions.

Yangtze River, inferred from the modal grain size of the fine silt fraction from core MD06-3040 (Wang et al., 2014; Figure 1), leads to the increased volume of material transported by the CDW (Yang et al., 1992; Li et al., 2007). Meanwhile, the intensified EAWM would increase southward transportation of material deposited in the YRE by the ECS coastal current (Liu et al., 2007). In addition, we observe that the main phases of increased FC_{32}1,15-diol proxy in core T06 coincide well with intervals of increased Asian dust emissions at 850–750 and 540–370 yr BP (Chen et al., 2020; Figures 4A, E). A marked increase in dust storm activity is related to an enhanced EAWM (Yang et al., 2022; Figures 4C, E). In conclusion, our study indicates that the EAWM and CDW are the main mechanisms controlling riverine OM input into the Yangtze River since the last 1000 years.

Although the terrestrial realm is an important source of OM to the ECS, it shows a spatial limitation. The trend of FC_{32}1,15-diol values in core T08 is inconsistent with records of EAWM intensity or Yangtze River discharge. For example, during the 900–600 yr BP interval, FC_{32}1,15-diol values decrease and then increase in core T08, showing an opposite trend to that of EAWM intensity (Xiao et al., 2004; Figures 4B, C). Furthermore, during the period of 500–300 yr BP, FC_{32}1,15-diol values fluctuate, while the Yangtze River discharge and the strength of the EAWM increase (Xiao et al., 2004; Wang et al., 2014; Figures 4B–D). Since core T08 is away from the YRE, terrestrial OM input has less influence on it in comparison to core T06.

4.3 Comparison of organic geochemical indicators in the ECS

Previous studies have suggested that natural features such as upwelling, CDW, and East Asian Monsoon (EAM) exert some of the major controls on marine ecology in the study region (Xing et al., 2011; Wang et al., 2012; Duan et al., 2014; Xing et al., 2016; Cao et al., 2017; Wang et al., 2019; Guo et al., 2020). Here, we assume upwelling is associated with increased phytoplankton productivity which is reconstructed by the sum of the concentrations of brassicasterol, dinosterol, and C_{37} alkenones ($\Sigma(A + B + D)$) (Wu et al., 2018; Wang et al., 2019). We find that downcore variations in $\Sigma(A + B + D)$ values in cores T08, F11A, F10C, and B3-1A are similar to DI-2 variations in core T08, all of which show an overall increasing trend during the past 1000 years (Figures 5Aa–e). For example, the relatively constant values in $\Sigma(A + B + D)$ and DI-2 during Period I, and significantly increased $\Sigma(A + B + D)$ values and DI-2 values during Period III (Wu et al., 2018; Wang et al., 2019; Figures 5Aa–e). This is attributed to a mechanism whereby enhanced KC activity and intensified upwelling supply a eutrophic environment that favors the growth of phytoplankton. However, during Period II, there are some differences between the $\Sigma(A + B + D)$ and DI-2 records. At this period, the DI-2 values decrease significantly, while no apparent variations in $\Sigma(A + B + D)$ values are observed in the four cores (Wu et al., 2018; Wang et al., 2019; Figures 5Aa-e). This could be interpreted that productivity changes are influenced by factors other than upwelling, such as the CDW (Duan et al., 2014; Cao et al., 2017; Guo et al., 2020) and the EAM (Wang et al., 2012; Cao et al., 2017). Therefore, the LCD based upwelling index provides a means to indirectly quantify the change in upwelling intensity for assessing the impact of upwelling on ecosystems, and plays a crucial role in future assessments and predictions of offshore fishery resources and ecological catastrophes.

Besides, the sources of terrestrial OM are various, including soils, terrestrial higher plants and rivers. The FC_{32}1,15-diol proxy can be used to infer riverine OM input and to distinguish the contribution of riverine OM (Lattaud et al., 2017a; Lattaud et al., 2017b). It is thought that the BIT index reflects the contribution of fluvial soil OM (Hopmans et al., 2004), and the LCA/MSCA and OEP proxies reflect the contribution of terrestrial higher plants to terrestrial OM input (Zheng et al., 2018). The comparison of FC_{32}1,15-diol proxy with other terrestrial proxies including TOC and $\delta^{13}C$ values, BIT index, LCA/MSCA ratio, and OEP proxy in the inner shelf of the ECS (Hu et al., 2014; Zheng et al., 2018; Zhou et al., 2020), indicates that only FC_{32}1,15-diol proxy has similar trend with TOC and $\delta^{13}C$ values during the past 1000 years (Figure 5B). This further indicates that terrestrial OM in the ECS originates from various sources and multiple proxies for terrestrial OM would be helpful to understand the past changes in terrestrial input in this region.

5 Conclusion

We generated diol proxies records in two sediments cores (cores T08 and T06) from the inner shelf of the ECS to investigate the evolution of the coastal upwelling system and terrestrial OM input in the area over the last millennium. At T08 station from the coastal upwelling area, the variations in DI-2 values are associated with the changes in the intensity of the EASM and the KC. During Period I (1000–600 yr BP), DI-2 values show a stable yet fluctuating trend, and the upwelling of the nutrient-rich KSSW is steady under the influence of a stable EASM. During Period II (600–400 yr BP), DI-2 values decrease significantly, with the lowest value at about 500 yr BP. The collaborative weakening of the EASM and KC would have meant that offshore movement of the upper layer of seawater is reduced and the nutrient contents of the bottom waters formed by the KSSW off the coast of Zhejiang also decrease. During Period III (from 400 yr BP to the present), when DI-2 values increase, the KC is relatively stable, and the strength of the EASM gradually increases; this would have meant that upward transportation of nutrients increases resulting from enhanced offshore movement of the upper layer of seawater.

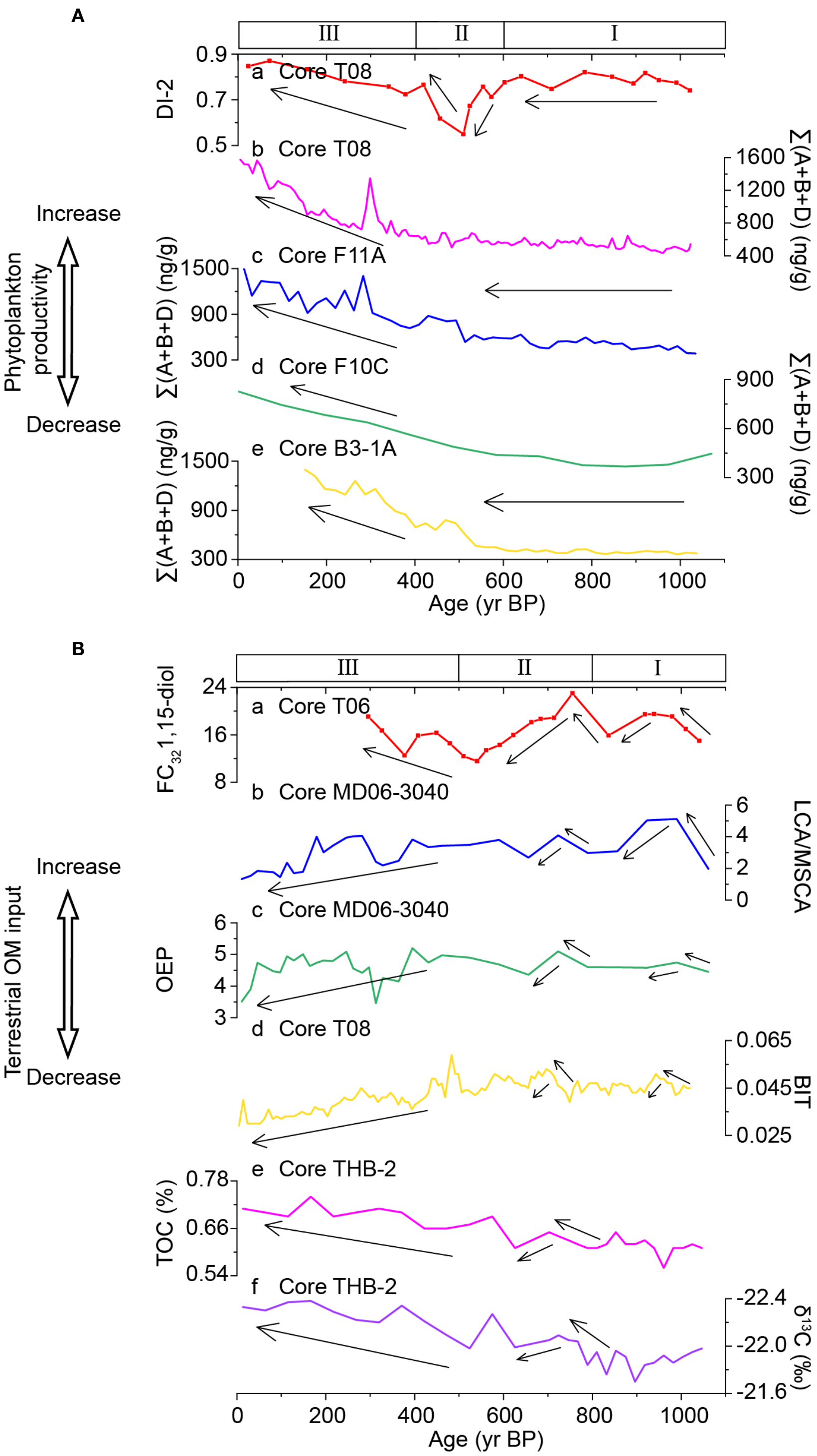

FIGURE 5
Organic geochemical indicators synthesis for reconstructing changes in upwelling intensity and tracing terrestrial OM input in the ECS. **(A)** Phytoplankton productivity records: **(a)** DI-2 record from core T08; ∑(A + B + D) records, (A,B,D refer to alkenones, brassicasterol, and dinosterol, respectively) used here to represent changes in phytoplankton productivity, from **(b)** core T08 (Wu et al., 2018), **(c)** core F11A (Wang et al., 2019), **(d)** core F10C (Wang et al., 2019), and **(e)** core B3-1A (Wang et al., 2019); **(B)** Terrestrial OM input records: **(a)** FC_{32}1,15-diol proxy in core T06; **(b)** LCA/MSCA ratio in core MD06-3040 (Zheng et al., 2018); **(c)** OEP proxy in core MD06-3040 (Zheng et al., 2018); **(d)** BIT index in core T08 (Zhou et al., 2020); **(e)** TOC values in core THB-2 (Hu et al., 2014); **(f)** $\delta^{13}C$ values in core THB-2 (Hu et al., 2014).

Additionally, fluctuations in DI-2 values in the core T08 show similar characteristics to changes in the Holocene ENSO index over the last millennium. This suggests that the increased frequency and intensity of ENSO events may strengthen upwelling along the Zhejiang and Fujian coasts.

At T06 station near to the YRE, FC_{32}1,15-diol variations are linked with the changes in the intensity of the EAWM and Yangtze River discharge during the past 1000 years. During Period I (1000–800 yr BP), FC_{32}1,15-diol values increase and then decrease, with high values corresponding well to intervals of strengthened EAWM; a stronger EAWM would have promoted southward transportation of material deposited in the YRE by the ECS coastal current. During Period II (800–500 yr BP), FC_{32}1,15-diol values decrease significantly and the EAWM strength declines; weakening of the EAWM would have led to a decrease in southward transportation along the ECS coast. During Period III (500–300 yr BP), FC_{32}1,15-diol values increase. During this period, intensified Yangtze River discharge would have caused an increase in the volume of material stored in the estuary, and the stronger EAWM would have elevated the southward transportation of materials deposited in the YRE by the ECS coastal current. In addition, intensified Asian dust emissions would have generated increasing amounts of sediments for eolian transportation during the past 1000 years, which leads to greater terrestrial OM input.

Data availability statement

The raw data supporting the conclusions of this article will be made available by the authors, without undue reservation. The raw data can be found in the Supplementary Material.

Author contributions

CS: Writing - Original draft preparation, Data curation, Validation. TD: Methodology, Measurement. TZ: Investigation. TG: Investigation. RoX: Core Dating. LX: Conceptualization, Supervision, Writing - Review and Editing. RB: Supervision, Writing - Review and Editing. YZ: Methodology. RuX: Writing Editing. BW: Figure Editing. All authors contributed to the article and approved the submitted version.

Funding

This study is funded by the National Natural Science Foundation of China (41876073, 92058207, and 42076037), the National Basic Research Program of China (973 Program 2010CB428901) and the Fundamental Research Funds for the Central Universities (Grant: 2020042010). This paper is also granted Taishan Young Scholars (Grant: tsqn202103030) and Shandong Natural Science Foundation (Grant: ZR2021JQ12).

Acknowledgments

We appreciate the constructive comments from the associate editor Prof. Zhaohui Zhang and two reviewers. We would like to thank the South China Sea Institute of Oceanography, Chinese Academy of Sciences and Peking University for their support of ^{14}C age dating.

Conflict of interest

The authors declare that the research was conducted in the absence of any commercial or financial relationships that could be construed as a potential conflict of interest.

Publisher's note

Supplementary material

The Supplementary Material for this article can be found online at: https://www.frontiersin.org/articles/10.3389/fmars.2022.1027561/full#supplementary-material

References

Balzano, S., Lattaud, J., Villanueva, L., Rampen, S. W., Brussaard, C. P. D., van Bleijswijk, J., et al. (2018). A quest for the biological sources of long chain alkyl diols in the western tropical north Atlantic ocean. *Biogeosciences* 15, 5951–5968. doi: 10.5194/bg-15-5951-2018

Beardsley, R. C., Limeburner, R., Yu, H., and Cannon, G. A. (1985). Discharge of the changjiang (Yangtze river) into the East China Sea. *Cont. Shelf. Res.* 4, 57–76. doi: 10.1016/0278-4343(85)90022-6

Cao, Y. Y., Xing, L., Zhang, T., and Liao, W.-H. (2017). Multi-proxy evidence for decreased terrestrial contribution to sedimentary organic matter in coastal areas of the East China Sea during the past 100 years. *Sci. Total. Environ.* 599, 1895–1902. doi: 10.1016/j.scitotenv.2017.05.159

Chen, F. H., Chen, S. Q., Zhang, X., Chen, J. H., Wang, X., Gowan, E. J., et al. (2020). Asian Dust-storm activity dominated by Chinese dynasty changes since 2000 BP. *Nat. Commun.* 11, 1–7. doi: 10.1038/s41467-020-14765-4 de Bar, M. W., Dorhout, D. J. C., Hopmans, E. C., Rampen, S. W., Sinninghe Damsté, J. S., and Schouten, S. (2016). Constraints on the application of long chain diol proxies in the Iberian Atlantic margin. *Org. Geochem.* 101, 184–195. doi: 10.1016/j.orggeochem.2016.09.005

de Bar, M. W., Hopmans, E. C., Verweij, M., Dorhout, D. J. C., Sinninghe Damsté, J. S., and Schouten, S. (2017). Development and comparison of chromatographic methods for the analysis of long chain diols and alkenones in biological materials and sediment. *J. Chromatogr. A.* 1521, 150–160. doi: 10.1016/j.chroma.2017.09.037

Ding, Z. X. (1983). Influence of wind on vertical structures of temperature and salinity, and upwelling off the zhejiang coast. *Oceanolog. Limnol. Sin.* 14, 14–21 (in Chinese).

Duan, S. S., Xing, L., Zhang, H. L., Feng, X. W., Yang, H. L., and Zhao, M. X. (2014). Upwelling and anthropogenic forcing on phytoplankton productivity and community structure changes in the zhejiang coastal area over the last 100 years. *Acta Oceanol. Sin.* 33, 1–9. doi: 10.1007/s13131-014-0535-1

Goñi, M. A., Ruttenberg, K. C., and Eglinton, T. I. (1998). A reassessment of the sources and importance of land-derived organic matter in surface sediments from the gulf of Mexico. *Geochim. Cosmochim. Acta* 62, 3055–3075. doi: 10.1016/S0016-7037(98)00217-8

Guo, Z. G., Yang, Z. S., Fan, D. J., and Pan, Y. J. (2003). Seasonal variation of sedimentation in the changjiang estuary mud area. *J. Geogr. Sci.* 13, 348–354. doi: 10.1007/BF02837510

Guo, X. Y., Zhang, H. L., Li, L., and Bi, R. (2020). Biomarker records of phytoplankton productivity and community structure changes in the mud area of the Yangtze river estuary in the East China Sea during the last 30 years. *J. OCEAN. Univ.* 50, 85–94 (in Chinese). doi: 10.16441/j.cnki.hdxb.20190164

Hedges, J. I., Keil, R. G., and Benner, R. (1997). What happens to terrestrial organic matter in the ocean? *Org. Geochem.* 27, 195–212. doi: 10.1016/S0146-6380(97)00066-1

He, L. H., Kang, M. Y., Zhang, D. R., and Jia, G. D. (2020). Evaluation of environmental proxies based on long chain alkyl diols in the East China Sea. *Org. Geochem.* 139, 1–11. doi: 10.1016/j.orggeochem.2019.103948

Hong, H. S., Zhang, C. Y., Shang, S. L., Huang, B. Q., Li, Y. H., Li, X. D., et al. (2009). Interannual variability of summer coastal upwelling in the Taiwan strait. *Cont. Shelf. Res.* 29, 479–484. doi: 10.1016/j.csr.2008.11.007

Hopmans, E. C., Weijers, J. W. H., Schefuß, E., Herfort, L., Sinninghe Damsté, J. S., and Schouten, S. (2004). A novel proxy for terrestrial organic matter in sediments based on branched and isoprenoid tetraether lipids. *Earth Planet. Sci. Lett.* 224, 107–116. doi: 10.1016/j.epsl.2004.05.012

Hu, D. X. (1994). Some striking features of circulation in huanghai Sea and East China Sea. *Oceanol. China Seas.* 1, 27–38. doi: 10.1007/978-94-011-0862-1_4

Hu, B. Q., Li, J., Zhao, J. T., Wei, H. L., Yin, X. J., Li, G. G., et al. (2014). Late Holocene elemental and isotopic carbon and nitrogen records from the East China Sea inner shelf: Implications for monsoon and upwelling. *Mar. Chem.* 162, 60–70. doi: 10.1016/j.marchem.2014.03.008

Hu, D. X., Lu, L. H., Xiong, Q. C., Ding, Z. X., and Sun, S. C. (1980). Study on the upwelling along the coast of zhejiang. *Sci. Bull.* 25, 131–133 (in Chinese).

Jian, Z. M., Wang, P. X., Saito, Y., Wang, J. L., Pflaumann, U., Oba, T., et al. (2000). Holocene Variability of the kuroshio current in the Okinawa trough, northwestern pacific ocean. *Earth Planet. Sci. Lett.* 184, 305–319. doi: 10.1016/S0012-821X(00)00321-6

Jing, Z. Y., Qi, Y. Q., and Hua, Z. L. (2007). Numerical study on upwelling and its seasonal variation along fujian and zhejiang coast. *J. Hohai. Univ.* 35, 464–470 (in Chinese).

Kong, G. S., and Lee, C. W. (2005). Marine reservoir corrections (ΔR) for southern coastal waters of Korea. *J. Korean. Soc. Oceanogr.* 10, 124–128. doi: G704-000255.2005.10.2.003

Kuo, N.-J., Zheng, Q. A., and Ho, C.-R. (2004). Response of Vietnam coastal upwelling to the 1997–1998 ENSO event observed by multisensor data. *Remote Sens. Environ.* 89, 106–115. doi: 10.1016/j.rse.2003.10.009

Lattaud, J., Dorhout, D., Schulz, H., Castañeda, I. S., Schefuß, E., Sinninghe Damsté, J. S., et al. (2017a). The C_{32} alkane-1,15-diol as a proxy of late quaternary riverine input in coastal margins. *Clim. Past.* 13, 1049–1061. doi: 10.5194/cp-13-1049-2017

Lattaud, J., Kim, J.-H., De Jonge, C., Zell, C., Sinninghe Damsté, J. S., and Schouten, S. (2017b). The C_{32} alkane-1,15-diol as a tracer for riverine input in coastal seas. *Geochim. Cosmochim. Acta* 202, 146–158. doi: 10.1016/j.gca.2016.12.030

Lee, H.-J., and Chao, S.-Y. (2003). A climatological description of circulation in and around the East China Sea. *Deep-Sea. Res. Part II-Top. Stud. Oceanogr.* 50, 1065–1084. doi: 10.1016/S0967-0645(03)00010-9

Lie, H.-J., Cho, C.-H., Lee, J.-H., and Lee, S. (2003). Structure and eastward extension of the changjiang river plume in the East China Sea. *J. Geophys. Res.-Oceans.* 108, 1–14. doi: 10.1029/2001JC001194

Liu, J. P., Xu, K. H., Li, A. C., Milliman, J. D., Velozzi, D. M., Xiao, S. B., et al. (2007). Flux and fate of Yangtze river sediment delivered to the East China Sea. *Geomorphology* 85, 208–224. doi: 10.1016/j.geomorph.2006.03.023

Li, M. T., Xu, K. Q., Watanabe, M., and Chen, Z. Y. (2007). Long-term variations in dissolved silicate, nitrogen, and phosphorus flux from the Yangtze river into the East China Sea and impacts on estuarine ecosystem. *Estuar. Coast. Shelf. Sci.* 71, 3–12. doi: 10.1016/j.ecss.2006.08.013

Luo, Y. Y., and Yu, G. Y. (1998). Numerical studies of wind and TWC-driven upwelling in coastal areas of the East China Sea. *J. OCEAN. Univ.* 28, 536–542. (in Chinese) doi: 10.1088/0256-307X/15/3/016

Mao, H. L., Ren, Y. W., and Wan, K. M. (1964). A preliminary investigation on the application of using T-s diagrams for a quantitative analysis of the watermasses in the shallow water area. *Oceanolog. Limnol. Sin.* 6, 1–22. (in Chinese)

Meyers, P. A. (1997). Organic geochemical proxies of paleoceanographic, paleolimnologic, and paleoclimatic processes. *Org. Geochem.* 27, 213–250. doi: 10.1016/S0146-6380(97)00049-1

Moy, C. M., Seltzer, G. O., Rodbell, D. T., and Anderson, D. M. (2002). Variability of El Niño/Southern oscillation activity at millennial timescales during the Holocene epoch. *Nature* 420, 162–165. doi: 10.1038/nature01194

O'Leary, M. H. (1988). Carbon isotopes in photosynthesis. *Bioscience* 38, 328–336. doi: 10.2307/1310735

Rampen, S. W., Datema, M., Rodrigo-Gámiz, M., Schouten, S., Reichart, G.-J., and Sinninghe Damsté, J. S. (2014a). Sources and proxy potential of long chain alkyl diols in lacustrine environments. *Geochim. Cosmochim. Acta* 144, 59–71. doi: 10.1016/j.gca.2014.08.033

Rampen, S. W., Friedl, T., Rybalka, N., and Thiel, V. (2022). The long chain diol index: A marine palaeotemperature proxy based on eustigmatophyte lipids that records the warmest seasons. *PNAS* 119, 1–11. doi: 10.1073/pnas.2116812119

Rampen, S. W., Schouten, S., Koning, E., Brummer, G.-J. A., and Sinninghe Damsté, J. S. (2008). A 90 kyr upwelling record from the northwestern Indian ocean using a novel long-chain diol index. *Earth Planet. Sci. Lett.* 276, 207–213. doi: 10.1016/j.epsl.2008.09.022

Rampen, S. W., Schouten, S., Wakeham, S. G., and Sinninghe Damsté, J. S. (2007). Seasonal and spatial variation in the sources and fluxes of long chain diols and mid-chain hydroxy methyl alkanoates in the Arabian Sea. *Org. Geochem.* 38, 165–179. doi: 10.1016/j.orggeochem.2006.10.008

Rampen, S. W., Willmott, V., Kim, J.-H., Rodrigo-Gámiz, M., Uliana, E., Mollenhauer, G., et al. (2014b). Evaluation of long chain 1,14-alkyl diols in marine sediments as indicators for upwelling and temperature. *Org. Geochem.* 76, 39–47. doi: 10.1016/j.orggeochem.2014.07.012

Rampen, S. W., Willmott, V., Kim, J.-H., Uliana, E., Mollenhauer, G., Schefuß, E., et al. (2012). Long chain 1,13- and 1,15-diols as a potential proxy for palaeotemperature reconstruction. *Geochim. Cosmochim. Acta* 84, 204–216. doi: 10.1016/j.gca.2012.01.024

Sinninghe Damsté, J. S., Rampen, S., Irene, W., Rijpstra, C., Abbas, B., Muyzer, G., et al. (2003). A diatomaceous origin for long-chain diols and mid-chain hydroxy methyl alkanoates widely occurring in quaternary marine sediments: Indicators for high-nutrient conditions. *Geochim. Cosmochim. Acta* 67, 1339–1348. doi: 10.1016/S0016-7037(02)01225-5

Stuiver, M., and Reimer, P. J. (2016). Extended ^{14}C data base and revised CALIB 3.0 ^{14}C age calibration program. *Radiocarbon* 35, 215–230. doi: 10.1017/S0033822200013904

Versteegh, G. J. M., Bosch, H.-J., and De Leeuw, J. W. (1997). Potential palaeoenvironmental information of C_{24} to C_{36} mid-chain diols, keto-ols and mid-chain hydroxy fatty acids; a critical review. *Org. Geochem.* 27, 1–13. doi: 10.1016/S0146-6380(97)00063-6

Wang, B. D. (1998). On the extension and nutrient transportation of the changjiang river diluted water. *J. Oceanogr. Huanghai. Bohai. Seas.* 16, 41–47 (in Chinese).

Wang, Y. J., Cheng, H., Edwards, R. L., He, Y. Q., Kong, X. G., An, Z. S., et al. (2005). The Holocene Asian monsoon: Links to solar changes and north Atlantic climate. *Science* 308, 854–857. doi: 10.1126/science.1106296

Wang, X.-C., Sun, M.-Y., and Li, A.-C. (2008). Contrasting chemical and isotopic compositions of organic matter in changjiang (Yangtze river) estuarine and East China Sea shelf sediments. *J. Oceanogr.* 64, 311–321. doi: 10.1007/s10872-008-0025-1

Wang, Z. C., Xiao, X. T., Yuan, Z. N., Wang, F., Xing, L., Gong, X., et al. (2019). Air-sea interactive forcing on phytoplankton productivity and community structure changes in the East China Sea during the Holocene. *Glob. Planet. Change* 179, 80–91. doi: 10.1016/j.gloplacha.2019.05.008

Wang, F., Xing, L., Zhang, H. L., Zhang, T., Ding, L., Chen, W. F., et al. (2012). Applications of lipid biomarkers for reconstructing changes of phytoplankton ecological structure and terrestrial input in core DH5-1 from the shelf of the East China Sea during the last 150 years. *J. Ocean. Univ.* 42, 66–72 (in Chinese). doi: 10.16441/j.cnki.hdxb.2012.11.010

Wang, K., Zheng, H. B., Tada, R., Irino, T., Zheng, Y., Saito, K., et al. (2014). Millennial-scale East Asian summer monsoon variability recorded in grain size and provenance of mud belt sediments on the inner shelf of the East China Sea during mid-to late Holocene. *Quat. Int.* 349, 79–89. doi: 10.1016/j.quaint.2014.09.014

Willmott, V., Rampen, S. W., Domack, E., Canals, M., Sinninghe Damsté, J. S., and Schouten, S. (2010). Holocene Changes in *Proboscia* diatom productivity in shelf waters of the north-western Antarctic peninsula. *Antarct. Sci.* 22, 3–10. doi: 10.1017/S095410200999037X

Wu, X. N., Xing, L., Zhang, T., and Xiang, R. (2018). Mid-late Holocene changes in sedimentary organic matter on the inner shelf of the East China Sea. *J. Asian Earth Sci.* 154, 248–254. doi: 10.1016/j.jseaes.2017.12.006

Wu, Y., Zhang, J., Liu, S. M., Zhang, Z. F., Yao, Q. Z., Hong, G. H., et al. (2007). Sources and distribution of carbon within the Yangtze river system. *Estuar. Coast. Shelf. Sci.* 71, 13–25. doi: 10.1016/j.ecss.2006.08.016

Xiao, S. B., Li, A. C., Chen, M. H., Liu, J. P., Jiang, F. Q., Li, T. G., et al. (2005). Recent 8 ka mud records of the East Asian winter monsoon from the inner shelf of the East China Sea. *J. China Univ. Geosci.* 30, 573–581 (in Chinese).

Xiao, S. B., Li, A. C., Jiang, F. Q., Li, T. G., Huang, P., and Xu, Z. K. (2004). Recent 2000-year geological records of mud area in the inner shelf of the East China Sea and their climatic implications. *Sci. Bull.* 49, 2233-2238 (in Chinese).

Xing, L., Zhang, R. P., Liu, Y. G., Zhao, X. C., Liu, S. M., Shi, X. F., et al. (2011). Biomarker records of phytoplankton productivity and community structure changes in the Japan Sea over the last 166 kyr. *Quat. Sci. Rev.* 30, 2666–2675. doi: 10.1016/j.quascirev.2011.05.021

Xing, L., Zhao, M. X., Zhang, T., Yu, M., Duan, S. S., Zhang, R. P., et al. (2016). Ecosystem responses to anthropogenic and natural forcing over the last 100 years in the coastal areas of the East China Sea. *Holocene* 26, 1–9. doi: 10.1177/0959683615618248

Xu, J. P. (1986). Preliminary analysis of the hydrologic structure in the coastal upwelling area off zhejiang in winter. *Donghai. Mar. Sci.* 4, 18–24 (in Chinese).

Yang, Z. S., Guo, Z. G., Wang, Z. X., Xu, J., and Gao, W. (1992). Basic pattern of transport of suspended matter from the yellow Sea and East China Sea to the eastern deep seas. *Acta Oceanol. Sin.* 14, 81–90 (in Chinese).

Yang, Y., Piper, D. J. W., Xu, M., Gao, J. H., Jia, J. J., Normandeau, A., et al. (2022). Northwestern pacific tropical cyclone activity enhanced by increased Asian dust emissions during the little ice age. *Nat. Commun.* 13, 1–12. doi: 10.1038/s41467-022-29386-2

Yang, D. Z., Yin, B. S., Liu, Z. L., and Feng, X. R. (2011). Numerical study of the ocean circulation on the East China Sea shelf and a kuroshio bottom branch northeast of Taiwan in summer. *J. Geophys. Res.-Oceans.* 116, 1–20. doi: 10.1029/2010JC006777

Yang, D. Z., Yin, B. S., Sun, J. C., and Zhang, Y. (2013). Numerical study on the origins and the forcing mechanism of the phosphate in upwelling areas off the coast of zhejiang province, China in summer. *J. Mar. Syst.* 123, 1–18. doi: 10.1016/j.jmarsys.2013.04.002

Zheng, B., Zhou, B., Wang, K., Pang, Y., Chen, M.-T., and Zheng, H. B. (2018). Changes of provenance input and source vegetation changes and their impact factors since late Holocene based on *n*-alkanes records from core MD06-3039A in the muddy area of the East China Sea. *Quaternary. Sci.* 38, 1293–1303 (in Chinese). doi: 10.11928/j.issn.1001-7410.2018.05.21

Zhou, Y., Wu, X. N., Xiang, R., and Xing, L. (2020). Decadal to interdecadal variability in TEX_{86} temperature on the inner shelf of the East China Sea over the last 3.7 kyr. *Org. Geochem.* 142, 1–9. doi: 10.1016/j.orggeochem.2020.104000

Zhu, X. W., Jia, G. D., Mao, S. Y., and Yan, W. (2018). Sediment records of long chain alkyl diols in an upwelling area of the coastal northern south China Sea. *Org. Geochem.* 121, 1–9. doi: 10.1016/j.orggeochem.2018.03.014